

Sandia National Laboratories
Waste Isolation Pilot Plant (WIPP)

Parameter Justification Report for DRSPALL

BOE 1.3.5.1.2.1

Effective Date: August 11, 2003

F. D. Hansen and T.W. Pfeifle
Repository Performance and Certification Department 6822
D. L. Lord
Performance Assessment and Decision Analysis Department 6821
Sandia National Laboratories
Carlsbad, NM 88220

Sandia is a multiprogram laboratory operated by Sandia Corporation, a Lockheed Martin Company, for the United States Department of Energy's National Nuclear Security Administration under contract DE-AC04-94AL85000.

WIPP:1.3.5.1.2.1:DC:QA-L:Parameter Justification

TABLE OF CONTENTS

1.0	Introduction.....	5
2.0	Waste Properties	8
2.1	Biot’s Beta	12
2.2	Poisson’s Ratio.....	12
2.3	Cohesion and Friction Angle	13
2.4	Tensile Strength	15
2.5	Waste Particle Size	20
2.6	Waste Porosity	22
3.0	Drilling Parameters	24
3.1	Parameters from General Practice	24
3.2	Stop Drilling Exit Volume Rate and Stop Pumping Exit Volume Rate	26
	Background.....	26
	Implementation in DRSPALL	27
3.3	Drill Penetration Rate	28
3.4	Solids Volume Fraction and Viscosity Exponent	28
3.5	Drilling Damage Zone	29
3.6	Absolute Roughness of Pipe and Wellbore	30
	Background.....	31
	Implementation in DRSPALL	31
4.0	Other Factors.....	34
4.1	Ergun Equation – Fluidized Bed Transport	34
	Particle shape factor.....	35
	Implementation in DRSPALL	36
4.2	Atmospheric Pressure	37
4.3	Roof Elevation	38
4.4	Land Surface Elevation.....	39
4.5	In Situ Stress	40
4.6	Salt Density	40
5.0	References.....	41
6.0	Acknowledgement	44

LIST OF FIGURES

Figure 2.1. Actual waste disposed in WIPP Panel 1	9
Figure 2.2. Illustration of WIPP waste in pipe overpacks	10
Figure 2.3. Iron Remaining in WIPP from TBM Calculations.....	11
Figure 2.4. Triaxial compression test on Specimen S 14.....	13
Figure 2.5. Calculation of Cohesion and Friction Angle	14
Figure 2.6. Tensile Strengths Determined from Thick-walled Cylinder Tests.....	17
Figure 2.7. Brine Saturation in a waste panel at 1000 years.....	18
Figure 2.8. Brine saturation in a waste panel at 2000 years.	19
Figure 3.1. Schematic of typical borehole in the Delaware Basin.....	25
Figure 3.2. Schematic of drilling at bottom hole	30
Figure 3.3. Diagram reproduced from Moody (1944) showing roughness values for common engineering materials.....	33
Figure 4.1. Minimum fluidization velocity calculated by Ergun's equation (Eq. 4.1.1) as a function of shape factor, given input values shown in Table 4.2.	36

LIST OF TABLES

Table 1.1 New parameters used in DRSPALL code.....	7
Table 2.1 Maximum and minimum porosity values from the 2002 TBM replicate 1, scenario 1 BRAGFLO runs.	22
Table 4.1 Nomenclature for Fluidization Calculations.....	34
Table 4.2 Input parameter values for Ergun sensitivity to shape factor shown in Figure 4.1.	35
Table 4.3 Shape factor calculated for cylinders with selected aspect ratios (diameter/height). ...	36
Table 4.4 Roof Elevations at the Center of Each WIPP Waste Disposal Panel	39
Table A.1 Master Table of Physical Parameters Called in a Typical DRSPALL Execution	45
Table B.1 Supporting spreadsheet calculations for Figure 4.1.	47

LIST OF ACRONYMS

CTAC	Carlsbad Field Office Technical Assistance Contract
CCA	Compliance Certification Application
DDZ	Drilling Damage Zone
DOE QAPD	Department of Energy Quality Assurance Program Document
DRZ	Disturbed Rock Zone
MOC	Management and Operating Contractor
NRC	National Research Council
NWMP	Nuclear Waste Management Program
WIPP	Waste Isolation Pilot Plant
WRES	Washington Regulatory and Environmental Services
WTS	Washington TRU Solutions LLC

1.0 INTRODUCTION

The certification process for opening the Waste Isolation Pilot Plant (WIPP) in the United States required the DOE to model the consequences of inadvertent intrusion into the repository during drilling for natural resources (40CFR 194.33(c)). The WIPP facility is located in southeastern New Mexico at a depth of 655 m in a geologic setting that comprises a great thickness of predominantly bedded halite adjacent to the repository horizon. This region of the United States contains significant quantities of natural resources, such as potash, gas and oil. Regulations require that performance assessment analyses assume that conventional drilling methods will be used to exploit natural resources, and these considerations are used in analyses of a hypothetical drilling intrusion.

The conceptual model is based on the postulate that at some future date an exploratory drilling operation penetrates the site. As part of the regulatory requirements evaluating long-term isolation of radioactive waste in a deep geologic repository, numerical calculations of probabilistic future states of the repository must be conducted. These calculations consider possible physico-chemical processes that could occur in the disposal areas. Processes considered include degradation of waste materials, leading to generation of gas pressure and degradation by-products. Uncertainty in gas generation processes leads to concomitant uncertainty in repository pressures during the 10,000-year regulatory time frame. As described in this document, this uncertainty spans a range from roughly hydrostatic pressure (~8 MPa) to the lithostatic stress state (~15 MPa). Within the constraints of several material and repository parameters, degraded waste material could break off, or spall into the drill string and transport to the surface by expelling gas present in the repository. This document compiles parameters implemented in the analyses of the spall phenomena.

DRSPALL (from Direct Release Spall) consists of a set of algorithms embedded in a computer code that are intended to calculate the volume of WIPP solid waste subject to material failure and transport to the surface as a result of an inadvertent drilling intrusion. The code calculates coupled repository and wellbore transient multi-phase compressible fluid flow before, during, and after the drilling intrusion process. Mathematical models are included of bit penetration, multi-phase (mud, salt, waste, and gas) fluid flow in the well, fluid expulsion at the surface, coupling of the well and the drilled repository, repository spalling due to tensile failure, fluidized bed transport of failed waste, and repository internal gas flow. The wellbore model is one-dimensional with linear flow, while the repository model is one-dimensional with either spherical or cylindrical flow.

The flow portions of DRSPALL are based on the theory of one-dimensional, time-dependent compressible isothermal fluid flow. The wellbore and repository flows are coupled at a specified boundary by a set of conditions. Throughout the process, the drill bit can move downward as a function of time, removing salt or waste material. Flow in the well is treated as a compressible, viscous, multi-phase mixture of mud, gas, salt, and possibly waste solids. Flow in the repository is treated as viscous, compressible single-phase gas flow in a porous solid. The effects of

depressurization in terms of the stresses on the waste are treated using simple linear elastic theory to predict the possibility of tensile failure, and removal of waste by flowing gas is estimated using fluidized bed equations. At the cavity forming the repository-wellbore boundary (following penetration) waste solids freed by drilling, tensile failure, and associated fluidization may enter the wellbore flow stream. Between the well and the repository, flow is treated according to the state of penetration.

This document relies extensively on reference material including the most recent considerations associated with the technical baseline migration and Option D panel closure effects (Stein and Zelinski, 2003a, 2003b). Parameters are discussed in three categories: waste characteristics, drilling practices, and other factors. Previous work (Hansen et al., 1997) showed that parameter extremes most likely to be of importance to spalling releases are high repository gas pressure, low mechanical strength of the waste, small waste particle size (after failure), and low waste permeability. DRSPALL will implement some of these key parameters in a manner similar to the mechanistic approach described by Hansen and coworkers. These parameters are derived from considerations of evolution of the waste environment and are categorized as waste properties. Since conventional drilling practices are to be assumed, drilling parameters are derived from industry practice. In order to execute bounding conditions of the model, allowance is made for continuous mud pumping during drilling and continuous drilling after repository penetration. Although this is not an expected situation, driller intervention is precluded. Further, current drilling practice information is used to identify several parameters related to down-hole geometry, nozzle size, advance rate, pump rate, etc. Other properties documented for the DRSPALL analysis include generally acceptable data for elevations, in situ stresses, and other input constants. Appendix A contains a table of all the parameters implemented in calculations with DRSPALL, including physical constants, values imported from BRAGFLO runs, and the 26 parameters discussed in this report. Table 1.1 lists the 26 parameters for which this document was created, includes the recommended values, and provides the Section of this report where discussion of each parameter is presented.

Table 1.1 New parameters used in DRSPALL code

Parameters	Section	Value(s)
Waste	2	
Biot Beta	2.1	1.0
Poisson's Ratio	2.2	0.35 to 0.43
Cohesion	2.3	0.14 MPa
Friction Angle	2.3	45.8°
Tensile Strength	2.4	0.12 to 0.17 MPa
Particle Diameter	2.5	0.1 to 10 cm
Waste Porosity	2.6	0.35 to 0.66
Drilling	3	
Mud Pump Rate	3.1	0.016-0.024 m ³ /s
Pipe Inner Diameter	3.1	0.097 m
Bit Nozzle Number	3.1	3
Bit Nozzle Diameter	3.1	#14 (14/32 in = 0.011 m)
Stop Drilling Exit Volume Rate*	3.2	1000 m ³ /s
Stop Pumping Exit Volume Rate*	3.2	1000 m ³ /s
Drill Penetration Rate	3.3	2.93 × 10 ⁻³ to 5.93 × 10 ⁻³ m/s
Mud Slurry Viscosity	3.4	
Maximum Solids Volume Fraction		0.59 to 0.64
Solids Viscosity Exponent		-1.2 to -1.8
Drilling Damaged Zone	3.5	
Thickness		0.16 m
Permeability		10 ⁻¹³ -10 ⁻¹⁵ m ²
Absolute Roughness	3.6	
Steel Drill Pipe		5 × 10 ⁻⁵ m
Wellbore Wall		5 × 10 ⁻⁵ to 3.1 × 10 ⁻³ m
Other	4	
Shape Factor in Ergun Equation	4.1	0.1 to 1.0
Atmospheric Pressure at Sea Level	4.2	1.0177 × 10 ⁵ Pa
Roof Elevation	4.3	384.70 m
Land Elevation	4.4	1037.3 m
Far-field in situ Stress	4.5	14.9 MPa
Salt Density	4.6	2180 kg/m ³

*These values are set arbitrarily large to preclude operator intervention, however, discussion is retained in this document.

2.0 WASTE PROPERTIES

Creation of surrogate wastes and mechanical experiments were completed previously (Hansen et al., 1997). A summary of these results is given here, but no new testing was done to support the DRSPALL model. The waste parameters were developed for bounding conditions of rampant waste degradation. To establish lower bounds for tensile strength, performance calculation realizations were considered along with the baseline inventory available at that time to develop degraded waste surrogates. To be sure, the baseline inventory as described in Hansen et al., (1997) is being updated and documented for re-certification. Generally, the update is expected to change the percentages of various components. The uncertainty involved with selection of the utterly degraded components is believed to bracket or represent percentage changes to the waste inventory.

Site-related information, such as waste disposal architecture and rock mechanics response of the underground setting, suggested that the most likely evolution of the in situ material includes - crushing, compaction and entombment by the surrounding salt. The bulky nature of the compressed inventory makes liberation and transportation of radionuclides problematic. The waste inventory comprises massive steel components including 55-gallon barrels, standard waste boxes and thick steel pipe overpacks, as shown in Figures 2.1 and 2.2, respectively. Future waste forms might include waste drums which have been supercompacted to 2000 tonnes, and stored in overpacks. However, in the most extreme cases the expected processes of iron corrosion and microbial activity can result in predictions of extensive degradation. This end state represents a bounding condition for the waste, which provides a means to quantify the lowest strength conditions of the future state of the waste, and, as discussed below, is appropriate for representing the lower bound strength of degraded waste from uncompacted barrels and standard waste boxes. Other, denser, waste forms such as pipe overpacks and supercompacted drums may be expected to degrade and corrode to a much lesser extent, and therefore will have strength, porosity and permeability values which are much less conservative than those assumed for standard wastes.

The primary emphasis of the waste surrogate testing was devoted to quantifying tensile strength, although many other characteristics such as particle size, permeability, and heterogeneity will greatly influence potential spall release. Utilizing a projected inventory of waste materials placed in the repository and assuming extensive degradation, recipes (mixtures) for surrogate products were determined. Surrogate recipes derived from corrosion of 50% and 100% of the iron-based inventory were fabricated and mechanically tested using standard laboratory procedures. The rationale for waste surrogate specimens was developed from inventory estimates as described in Appendix A of Hansen et al. (1997). As testing proceeded, emphasis was given to the surrogate mixtures representing corrosion of 50% of the iron-based inventory because the performance assessment calculations show that amount or more remains (Figure 2.3). Subsurface processes leading to extreme degradation are based on several contributing conditions including ample brine availability, extensive microbial activity, corrosion, and the absence of cementation and salt encapsulation effects.



Figure 2.1. Actual waste disposed in WIPP Panel 1



Figure 2.2. Illustration of WIPP waste in pipe overpacks

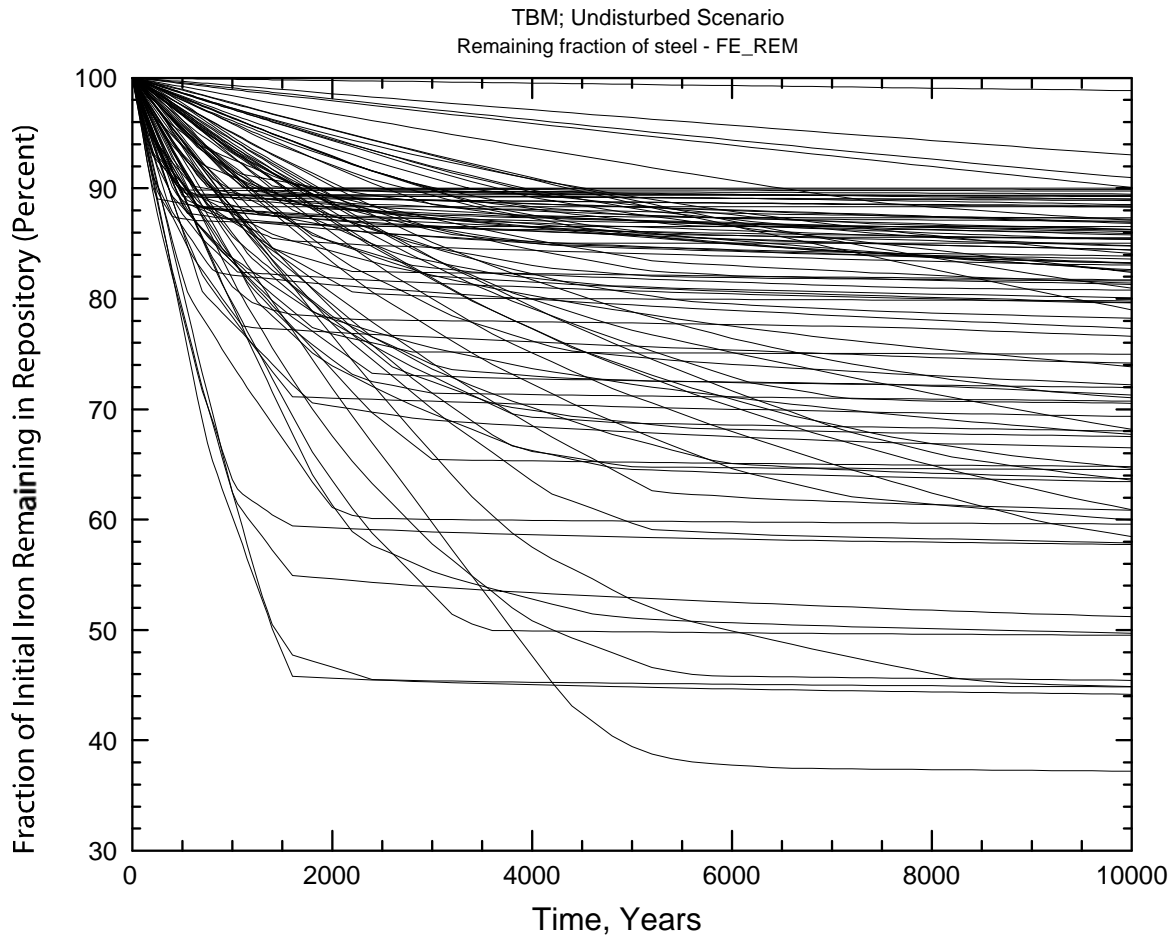


Figure 2.3. Iron Remaining in WIPP from TBM Calculations

The remainder of this section is devoted to waste properties used in calculations with DRSPALL. Strength and mechanical properties were derived from laboratory experiments on surrogate materials during preparation of the CCA. The records are filed in Sandia's Carlsbad Office under the Nuclear Waste Management Program (NWMP) Records Management Profile Package #252034 (DPRP1:NF Fabrication and Testing of Surrogate Degraded Waste Material, Task 20, AG-4911). Four property values implemented in DRSPALL were determined from experimental results obtained for surrogate degraded waste materials: Poisson's Ratio, Cohesion, Friction Angle and Tensile Strength. These material properties all derive from WIPP project reports and further information can be obtained from Hansen et al., (1997). The values for particle size were obtained via formal expert elicitation. Estimates of WIPP waste particle sizes based on the expert elicitation were prepared by Dr. Yifeng Wang (WPO# 46936). Biot's Beta is quantified from the technical literature as it applies to the spalling scenario.

2.1 Biot's Beta

The effective stress law defines a relationship for the interplay of confining stress and internal pore pressure, usually presented in the form:

$$P=G(\sigma - \beta p) \quad (2.1.1)$$

Where G is a generalized function that describes the effect of stress on the property, σ is the external stress, p is the pore pressure and β is the poroelastic parameter that relates stress and pore pressure. If $\beta=1.0$ the result is the classic effective stress law which is widely applied satisfactorily to soils and materials possessing relatively high permeability, say of the order of a darcy (10^{-12} m^2). The permeability ranges of concern for the spalling evaluation are in this neighborhood, consistent with assigning $\beta=1.0$. For example, the CCA baseline permeability for WIPP waste was estimated at a constant value of 10^{-13} m^2 (see Appendix A). In the DRSPALL conceptual model, a drilling damage zone is implemented as the drill bit nears the waste room (Section 3.5). It is expected that flow from the high-pressure repository into the wellbore will be bridged by a relatively permeable zone (sampled over a range of 10^{-13} to 10^{-15} m^2), which is also consistent with assignment of β equal to 1.0.

This conclusion is supported by experimental study, such as the review of the effective stress law for low-permeability rocks (Warpinski and Teufel, 1992). They report that samples that have more microcracks and slot porosity tend to reflect a β close to unity. This type of "slot" porosity is similar to the likely porosity of compacted waste, which includes 7-packs stacked three high with a hard plastic slip sheet placed horizontally between tiers. These considerations taken together suggest that 1.0 is the most likely value for Biot's Beta and this value would be conservative for failure since it maximizes the effect of pore pressure in reducing effective compression.

2.2 Poisson's Ratio

Tests on surrogates emphasized tensile strength, but some triaxial and uniaxial tests were also conducted (Hansen, et al., 1997). Measurements of compressive strength included both stress and strain measurements, thus providing estimates for Poisson's Ratio along with other properties of interest (even though they are not included in the current DRSPALL model). Surrogate samples were ductile in both tension and compression as exhibited by the triaxial compression test plotted in Figure 2.4. The drained test was performed at room temperature using a constant confining pressure of 1 MPa. The load path incorporated two unload/reload cycles, which provided information for estimating the two elastic constants: Young's Modulus and Poisson's Ratio.

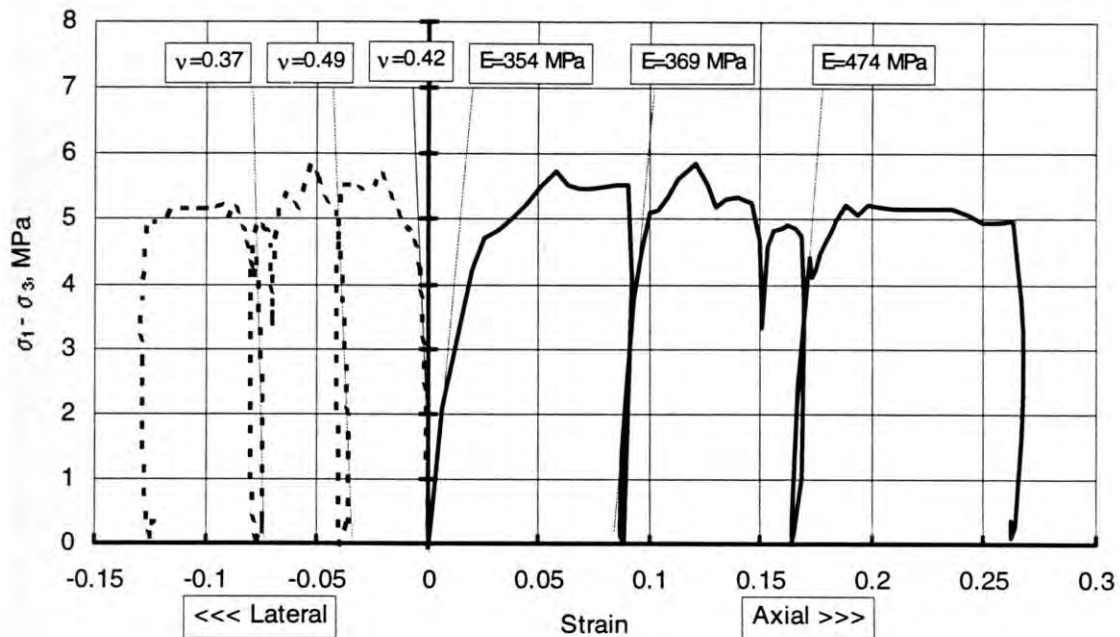


Figure 2.4. Triaxial compression test on Specimen S 14

Young's Modulus was calculated from the slope of the axial stress difference versus axial strain data during the ascending load portions of the curve. Poisson's Ratio was calculated by first calculating a similar slope for the axial stress difference versus lateral strain data during the ascending load portions of the curve. The ratio of Young's Modulus to this lateral strain slope represented Poisson's Ratio. Only three tests were conducted in this fashion and the average Poisson's Ratios determined thereby are 0.35, 0.35 and 0.43. It would be reasonable to use range of values from 0.35 to 0.43 for Poisson's Ratio, typical values for a fairly compliant material. It would be equally valid to assign $\nu = \text{constant } 0.38$.

Parameter name	Units	Low	High	Distribution
Poisson's ratio	-	0.35	0.43	Uniform

2.3 Cohesion and Friction Angle

These two parameters are used to describe typical pressure-dependent strength failure envelopes. Unconfined compressive strength calculates the stress at maximum load, corrected for instantaneous strain. Owing to the ductile nature of some surrogate waste specimens, load-bearing capacity was not always apparent. In such cases, tests were terminated after large strain accumulation and the corresponding load was used to calculate uniaxial strength. Seven unconfined compression tests were performed using the mixtures identified as 50% and 100% degraded waste (Hansen, et al., 1997. Five of those tests used specimens that were saturated with

brine, and two of the tests used specimens that had initially been saturated with brine, but were dried before testing commenced. The strength of the wet specimens ranged from 0.32 MPa to 1.4 MPa and averaged 0.75 MPa. The two dry specimens displayed strengths of 1.0 MPa and 1.3 MPa.

As discussed in the analog evaluations in Chapter 5 of Hansen et al. (1997), cohesion is an important parameter for cavity calculations pertaining to methane production. Sufficient test data were produced to allow determination of cohesion of surrogate materials. To capture the low-end strength results, saturated test results were used to estimate cohesion, C , and friction angle, ϕ . Saturated data were plotted as $(\sigma_1 - \sigma_3)/2$ versus $(\sigma_1 + \sigma_3)/2$ (i.e., in-plane shear stress vs. in-plane mean stress). These data plot linearly as shown in Figure 2.5. A line of the form of

$$\frac{(\sigma_1 - \sigma_3)}{2} = m \frac{(\sigma_1 + \sigma_3)}{2} + b \quad (2.3.1)$$

was fitted to the data. The fit is shown in Figure 5, where m and b are related to friction angle and cohesion as follows:

$$\phi = \arcsin(m) = 45.8^\circ \quad (2.3.2)$$

$$C = \frac{b}{\cos \phi} = 0.14 \text{ MPa}$$

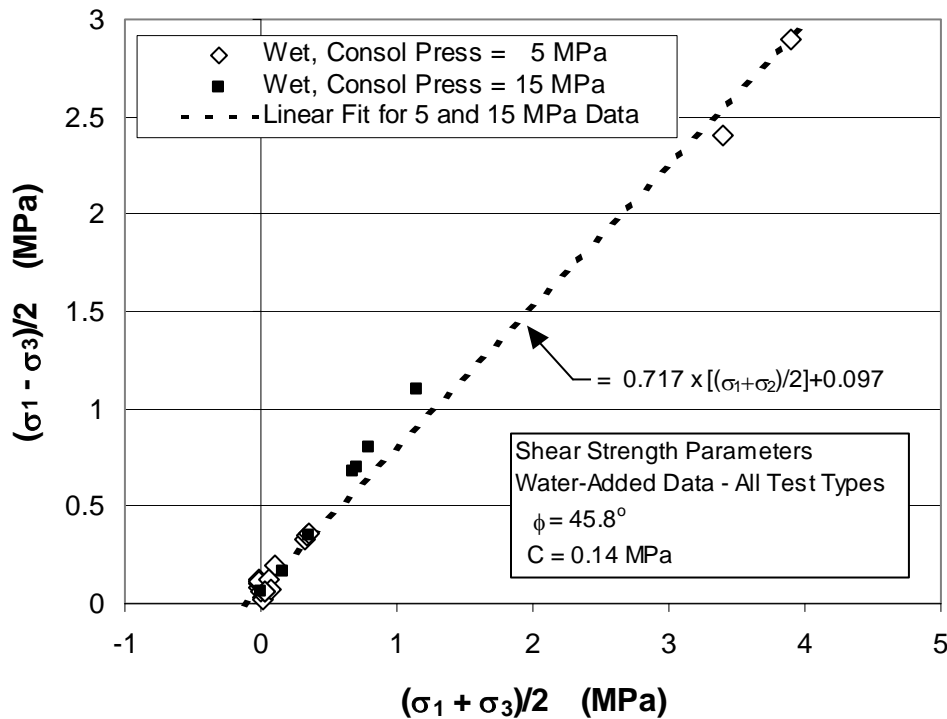


Figure 2.5. Calculation of Cohesion and Friction Angle

In a previous analysis (Hansen et al., 1997), ϕ was calculated to be 44.4° and C was calculated to be 0.13 MPa. The available results can be evaluated using the experimental data in various ways. Tests in Figure 2.5 are all saturated; when other tensile data are added to the analysis, ϕ and C are hardly affected because the fit to the data is anchored by the triaxial compression results. These strength data represent highly degraded, saturated surrogate samples and as such, they reflect relatively constant values at the lowest end of the strength scale.

2.4 Tensile Strength

Particular attention was given to determining tensile strength, because the initial work in the spallings model suggested that tensile strength was a parameter of paramount importance to performance assessment. Two techniques were used to investigate tensile strength for the surrogate waste samples: the Brazilian indirect method and hollow cylinders. These sample geometries were conducive to our specimen preparation apparatus. The Brazilian technique applies a compressive state to induce a tensile field, assuming an elastic solution. The indirect technique is probably satisfactory for partially dry (stiffer) surrogate waste; however, the saturated specimens were sufficiently ductile that tensile stress states predicted by elastic solutions might not be applicable. Therefore, an alternative test technique using hollow cylinders subjected to internal pressure was developed for most tensile strength values. The thick-walled cylinder tests were performed by pressurizing the cylinders over their internal surface without applying any external pressure or axial stress. With this configuration, the maximum tensile stress experienced by the specimen occurs at the surface of the inner wall and may be calculated.

Brazilian Indirect Tension Test Solution (Jaeger and Cook, 1976):

For the Brazilian test,

$$\sigma_1 = \sigma_{\text{diametral}} = \frac{6P}{\pi LD} \tag{2.4.1}$$

$$\sigma_3 = \sigma_{\text{tensile}} = T_o = -\frac{2P}{\pi LD}$$

where $\sigma_{\text{diametral}}$ is the compressive stress across the diameter of the specimen, T_o is the tensile strength, P is the diametral load, and L and D are the specimen length and diameter.

Thick-Walled Hollow Cylinder Solution (Jaeger and Cook, 1976):

For a thick-walled cylinder with no axial loading in the out-of-plane direction, the radial and circumferential stresses (σ_r and σ_θ) are expressed (using compression +) as:

$$\sigma_r = \frac{p_2 R_2^2 - p_1 R_1^2}{R_2^2 - R_1^2} - \frac{(p_2 - p_1) R_1^2 R_2^2}{r^2 (R_2^2 - R_1^2)} \quad (2.4.2)$$

$$\sigma_r = \frac{p_2 R_2^2 - p_1 R_1^2}{R_2^2 - R_1^2} + \frac{(p_2 - p_1) R_1^2 R_2^2}{r^2 (R_2^2 - R_1^2)}$$

where p_2 and p_1 are the external and internal pressures; R_2 and R_1 are the outer and inner radius; and r is the radius to some arbitrary point in the wall of the cylinder.

For the surrogate waste tests, $p_2 = 0$ and p_1 is the internal pressure applied by the expandable bladder. Under these conditions the maximum tension occurs when $r=R_1$, so the two equations become (also expressed as principal stresses σ_1 and σ_3 and tensile strength, T_o):

$$\sigma_1 = \sigma_r = p_1 \quad (2.4.3)$$

$$\sigma_3 = \sigma_\theta = T_o = -p_1 \frac{\left(1 + \frac{R_1^2}{R_2^2}\right)}{\left(1 - \frac{R_1^2}{R_2^2}\right)}$$

The bulk of the tensile strength testing was performed using thick-walled specimens because that geometry was considered better suited to achieve uniform loading of the material. Tensile strengths determined from the indirect tension tests were similar despite the less-than-optimal procedure.

Tensile strength data for 50% degraded surrogate are shown graphically in Figure 2.6, which plots tensile strengths versus the level of specimen saturation at the time of testing. These data indicate that tensile strength increases as moisture content decreases. Recommended values for tensile strength are selected based on performance assessment calculations, as discussed subsequently.

A set of PA calculations (AP106) was run for the Salado Flow Peer Review panel in February 2003 (Stein and Zelinski, 2003a, b). Figures 2.7 and 2.8 show scatter plots of brine saturation in the single waste panel versus pressure for the undisturbed scenario at 1,000 and 2,000 years for these calculations. The figures indicate that within the first 2,000 years (1) no vectors have saturations that exceed ~0.6 and (2) the vectors with the highest brine saturations have relatively low pressures. These results are different than what was calculated for the CCA and PAVT because of the inclusion of Option D panel closures in the AP106 runs.

In the CCA and PAVT, large amounts of brine could enter the waste areas from the northern experimental and operations areas because of the 1-degree dip to the south and the generic panel

closures modeled in these calculations were quite permeable. In the CCA and PAVT, the single waste panel could almost become fully saturated regardless of repository pressure. For the Technical Baseline Migration (TBM) (Hansen et al., 2002) and AP106 calculations, Option D panel closures were implemented in the BRAGFLO grid. These panel closures effectively blocked this brine pathway and resulted in drier conditions in the single waste panel. With the Option D panel closures implemented in the calculations it is evident that there is some correlation between brine saturation and pressure: higher pressure vectors tend to have lower brine saturations.

Based on these results, it would appear that the surrogate tensile strengths over the saturations between 0 and 50% would be justified and would narrow the bounds of uncertainty. Thus, a reasonable range for tensile strength would be 0.12 to 0.17 MPa.

Parameter name	Units	Low	High	Distribution
Tensile Strength of Waste	MPa	0.12	0.17	LogUniform

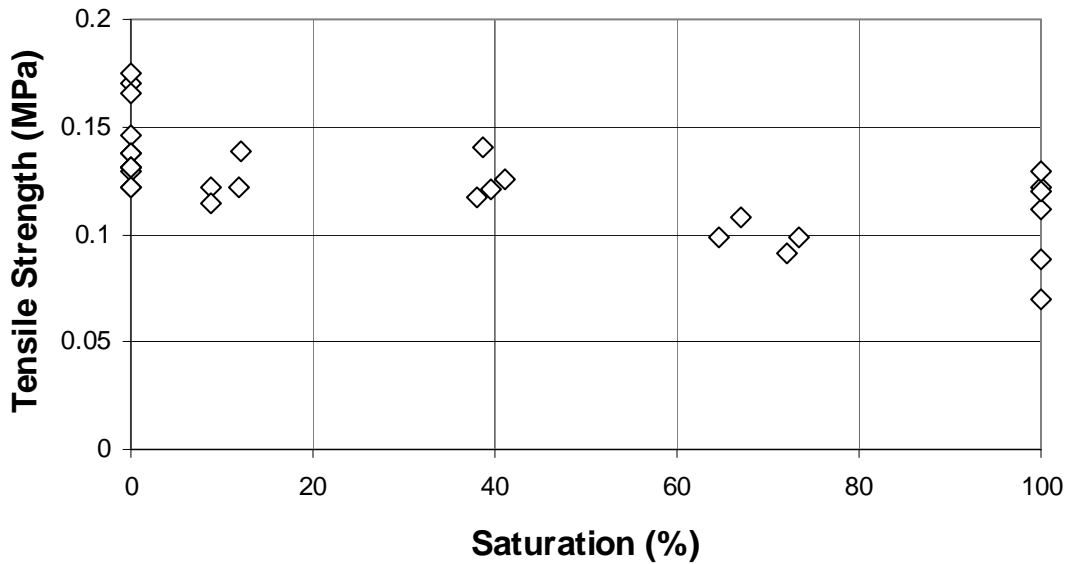


Figure 2.6. Tensile Strengths Determined from Thick-walled Cylinder Tests

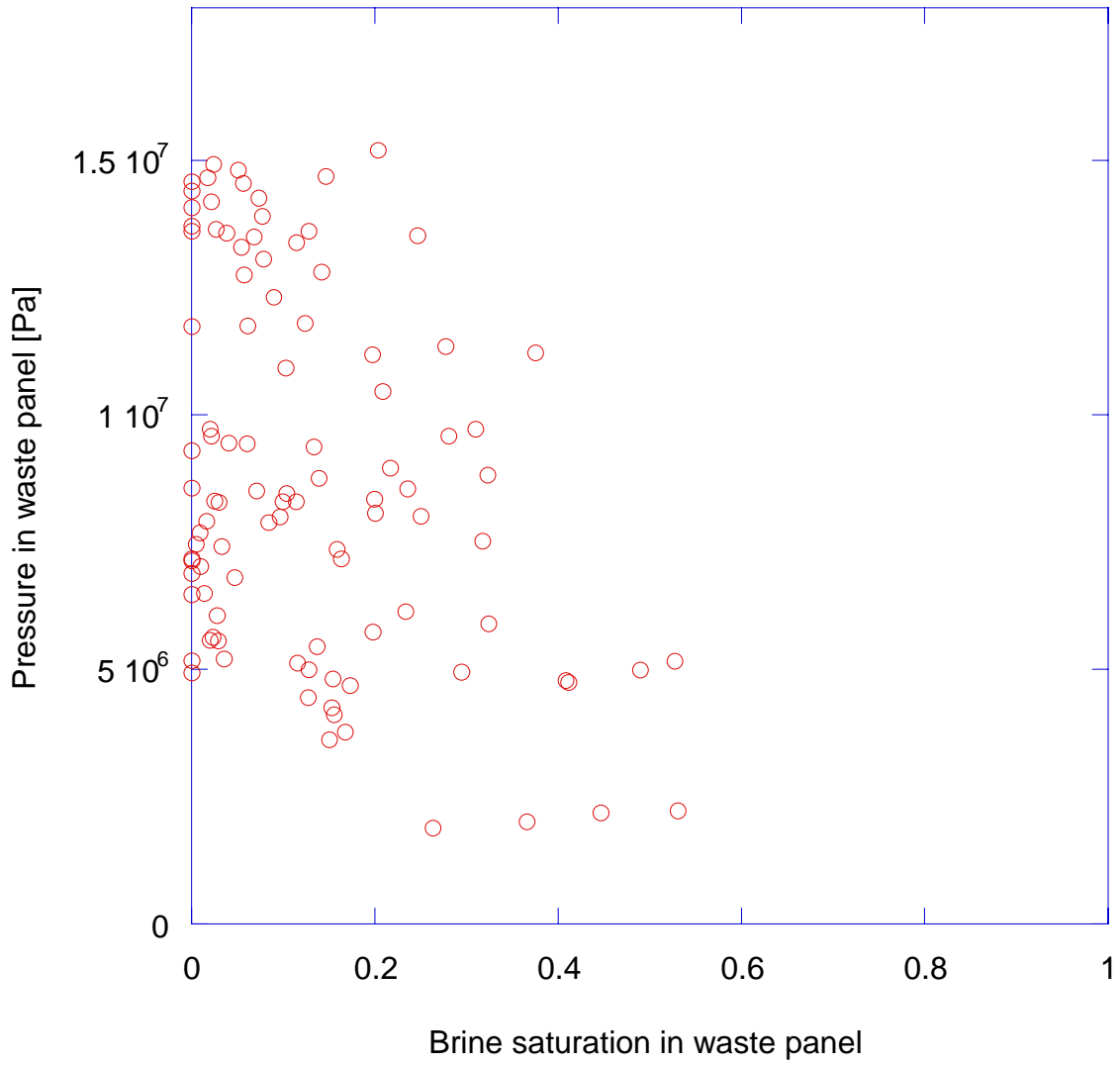


Figure 2.7. Brine Saturation in a waste panel at 1000 years.

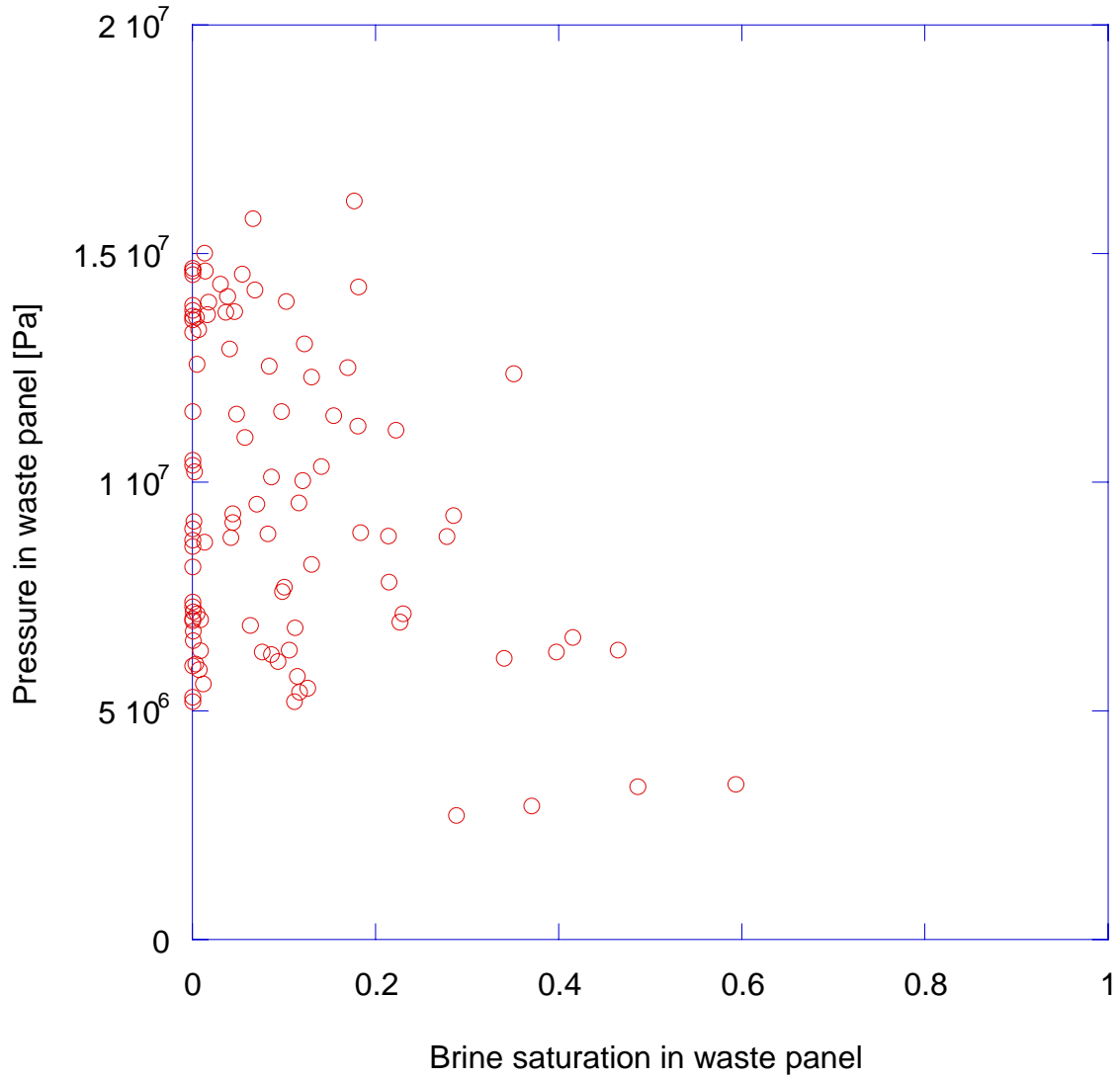


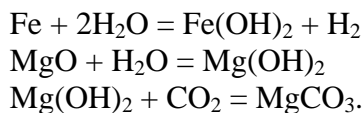
Figure 2.8. Brine saturation in a waste panel at 2000 years.

2.5 Waste Particle Size

An expert elicitation was conducted in 1997 on particle size distribution(s) of transuranic waste in the Waste Isolation Pilot Plant (WIPP) over the 10,000-year regulatory post-closure period (CTAC, 1997). The elicitation results consisted of a model for predicting waste particle size. According to chemical characteristics, the expert panel categorized WIPP transuranic waste into four groups: (1) iron- and aluminum-based metal/alloys, (2) cellulose/solidified organics, (3) rubber/plastics, and (4) other metals/ inorganic/vitrified/soils/cements/solidified inorganics. For each group, the initial distribution of particle size and particle number were specified. The expert panel included MgO backfill and salt as two additional waste groups, although those materials are not real wastes. Since the MgO pellets used for recent experimental studies have a size range of 0.5 to 4 mm (Sandia, 1997), the panel estimated that MgO backfill has a constant particle size of $\sim 10^{-9} \text{ m}^3$. The panel also estimated that the particle size of salt ranges from dust (1 μm in diameter) to half room size slabs (2 m thick), with an average value of 10^{-5} m^3 . The expert panel treated particles as equivalent spheres.

The expert panel also identified chemical and physical processes that can modify the particle sizes of the waste over the 10,000 year regulatory post-closure period. Those processes include crushing, anoxic metal corrosion, organic material biodegradation, precipitation/cementation, encapsulation, and fragmentation. Room creep closure will tend to crush the waste containers, exposing their contents to the surrounding environment to a variable extent. Crushing could result in mechanical bonding of waste as some components deform into interlocking shapes. During room closure, salt may creep locally into the voids in the waste, encapsulating waste particles.

Hydration and cementation are the two most important processes controlling the evolution of waste particle size in the repository. The chemical reactions involved in the two processes include:



Water consumption in the above reactions may also cause salt precipitation out of brine. The expert panel estimated that most corrosion and MgO hydration products would precipitate out as cementation agents, with the remainder precipitating as free particles. The panel assessed that a maximum of 25% of the reaction products would precipitate out as free particles, and that this percentage would decrease to zero as available porosity approaches zero. The free particles will range in size from 0.1 to 10 μm , with an average value of 2 μm . The expert panel suggested that smaller particles were likely to be aggregated by cement, with the likelihood approximately inversely proportional to particle volume. The panel estimated that the particle size would approach to room size (i.e. a cemented mass) as the cement volume approaches about 40% of pore space (assuming about a 25% porosity prior to cementation) and that the range of particle size will also decrease (CTAC, 1997).

Based on the expert elicitation result, Wang (1997) estimated the particle size distribution for degraded wastes. To be physically meaningful, Wang first converted a particle number-based distribution, specified by the expert panel, into a volume fraction-based distribution, because the waste volume is an important parameter in spalling and caving releases. Wang then quantified the effects of dissolution and cementation processes on waste particle size distributions. Waste particles can be reduced in size by various dissolution processes, such as that concomitant with steel corrosion and organic material biodegradation. However, the calculation shows that these dissolution processes will not produce any significant volume fraction of fine particles in the repository. As a matter of fact, dissolution tends even to eliminate small particles present in the initial wastes. Cementation was identified by the expert panel as an important process leading to the aggregation of waste particles in the repository. Based on the panel's assumption that the particle size would approach room size (i.e. a cemented mass) as the cement volume approaches about 40% of the available pore space, Wang demonstrated that cementation induced by either MgO hydration or steel corrosion, could effectively aggregate waste particles to a room size.

To calculate the lower limit of particle size distribution, Wang invoked a bounding case, in which fine particles precipitated during steel corrosion and MgO hydration were assumed to remain un-cemented with a diameter of 2 μm and no particle aggregation is assumed for partially-reacted and non-reactive waste components. The calculation shows that, even in this bounding case, particles smaller than 120 μm account for only 16% of total volume and 30% degradation of either steel or MgO will produce enough cements to raise the smallest particle size from 2 μm to > 120 μm . Therefore, in actual worst cases, particles smaller than 120 μm will account for less than 10% of total volume.

Wang further argued that, the appropriate particle size range must be estimated based on mean particle size, for the following reasons:

- A small fraction of fine particles can be present in the initial waste. However, there is no conceivable mechanism by which the fine particles will be segregated from coarse particles in space on a multiple-drum scale.
- The fine particles produced by MgO hydration and steel corrosion can be present only when MgO and steel are partially reacted, and thus those particles will be always mixed with remaining MgO and steel particles.
- Therefore, the fine particles not only account for a small fraction of total solid volume but will also remain mixed with large particles. From a mechanistic point of view, small particles cannot be eroded unless large particles become mobile.

There are various ways to define mean particle sizes. The most commonly used definitions are the arithmetic mean, the geometric mean, and the median. Wang calculated all three mean values for the lower bounding case. It was found that all three means were larger than 1 mm. Since cementation can effectively aggregate waste particles to a room size, and also because particles larger than the drill bit diameter cannot be released through a borehole, 0.1 m is recommended as the upper limit of mean particle size for the spalling and caving models. Therefore, Wang established the range of mean particle size to be 1mm to 10 cm.

2.6 Waste Porosity

This section documents the range of values selected for the waste intrinsic porosity, defined as the void volume divided by the current bulk volume, in the DRSPALL model. Porosity enters into DRSPALL in both the porous flow equations that govern compressible gas flow in the repository, as well as in the Ergun equation (Section 4.1) for fluidized bed transport of disaggregated waste material. While repository pressure and waste porosity for specific intrusions in the WIPP can potentially come directly from BRAGFLO output during compliance calculations, it is necessary to define a distribution of possible input values in order to execute a sensitivity study. Moreover, if the ultimate implementation of DRSPALL takes the form of a spillings response surface, this range must be defined in the event that it takes a primary role as an independent variable in the response function.

The range of possible input values for waste porosity was derived by examining BRAGFLO output from the 2002 Technical Baseline Migration study (Hansen et al., 2002). Volume-averaged waste porosity data for the intruded panel (WAS_POR) were extracted from the WIPP PA configuration Management System (CMS) for scenario 1, replicate 1. In general, the porosity of the waste area decreases rapidly during the first 500 years as creep closure collapses the repository, with minimum values typically seen around 2000 years. Between 2000 and 4000 years, the porosities increase slightly and then reach a steady-state value after 4000 years. The BRAGFLO porosity must be converted to intrinsic porosity using the following formula:

$$\phi = \frac{\phi_B}{\phi_B + (1 - \phi_o)} \quad (2.6.1)$$

where ϕ is the intrinsic waste porosity, ϕ_B is the BRAGFLO waste porosity, and ϕ_o is the initial waste porosity at the time of site closure. To define a representative range of values used in DRSPALL, porosity values at times of 350, 1000, 2000, and 10,000 years, with maximum and minimum values are summarized in Table 2.1.

Table 2.1 Maximum and minimum porosity values from the 2002 TBM

Time (yr)	Minimum BRAGFLO Porosity	Minimum Intrinsic Porosity	Maximum BRAGFLO Porosity	Maximum Intrinsic Porosity
350	0.117	0.435	0.298	0.662
1000	0.085	0.358	0.229	0.601
2000	0.082	0.349	0.226	0.598
10000	0.095	0.384	0.255	0.626

The minimum BRAGFLO porosity observed in the reported data was 0.082 at 2000 years, while the maximum was 0.298 at 350 years. The intrinsic waste porosity range therefore deemed appropriate for use in DRSPALL is as follows:

Minimum intrinsic porosity:	0.35
Maximum intrinsic porosity:	0.66

3.0 DRILLING PARAMETERS

3.1 Parameters from General Practice

Several parameters considered in implementation of the DRSPALL code involve dimensions of the drilling apparatus itself. The language in 40 CFR 194.33(c)(1) is:

(c) Performance assessments shall document that in analyzing the consequences of drilling events, the Department assumed that:

(1) Future drilling practices and technology will remain consistent with practices in the Delaware Basin at the time a compliance application is prepared. Such future drilling practices shall include, but shall not be limited to: the types and amounts of drilling fluids; borehole depths, diameters, and seals; and the fraction of such boreholes that are sealed by humans... (EPA, 1996)

The Delaware Basin Drilling Surveillance Program monitors the drilling practices in the vicinity of the Waste Isolation Pilot Plant in response to Environmental Protection Agency requirements. From the most recently available report (USDOE, 2002) some of the pertinent information regarding drilling practices is quoted below.

The DBDSP tracks borehole depths for all wells drilled in the Delaware Basin. Borehole depths in the immediate vicinity of the WIPP Site typically range from 8,000 to 9,000 feet for oil wells and 13,000 to 16,000 feet for gas wells. The diameter of each well bore is more difficult to ascertain. The DBDSP tracks the casing size and depth for each section of the hole. Drill bit size is not a reportable element, although hole sizes are sometimes reported on Sundry notices (miscellaneous forms) maintained by the New Mexico Oil Conservation Division (NMOCD). The casing size or hole size is used to determine the size of the bit used to drill that particular section of the well. Currently, the most common bit sizes being used are 17 1/2" for the surface section, 11" for the intermediate section, and 7 7/8" for the production section of the hole.

In the early days of well drilling, the 12 1/4" bit was popular with rotary drill operators for the surface section of the hole. In those days, the wells were much shallower and did not require the larger sections of casing. Most holes drilled at that time were a two-string (string refers to the different size of casing in the wellbore) hole versus the three- and four-strings commonly used now. In the area of the WIPP Site, regulations require a three-string hole making the larger bit sizes more popular. The typical hole and casing sizes for a three-string well in the vicinity of the WIPP Site are shown in Figure 3.1.

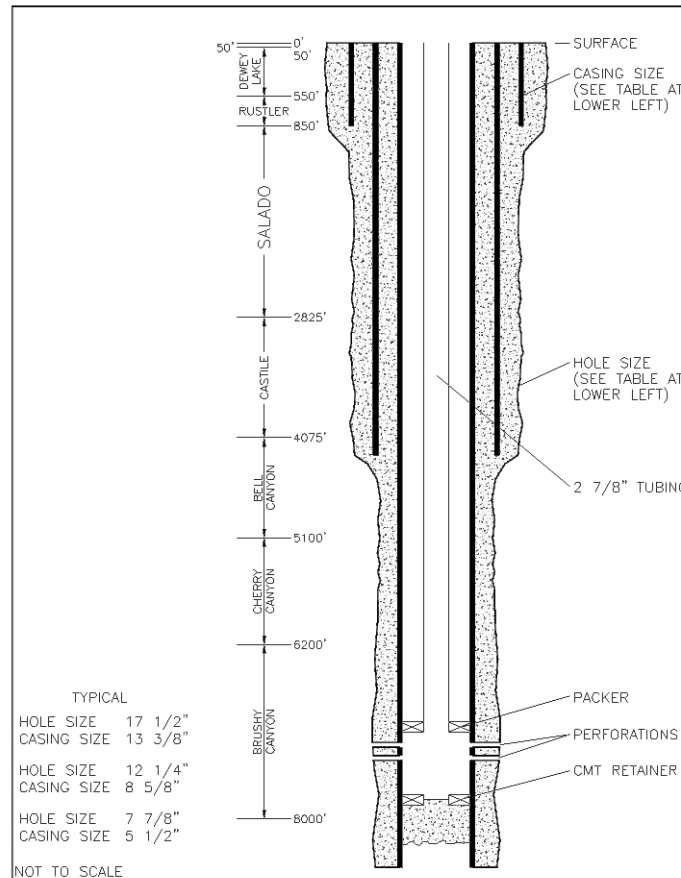


Figure 3.1. Schematic of typical borehole in the Delaware Basin.

The DBDSP information (USDOE, 2002) did not include all of the parameters sought for DRSPALL applications. According to David Hughes (2003) (see Appendix C) of Washington Regulatory Environmental Services LLC (WRES) the managing operating contractor at WIPP, characteristics such as drill bits and drill pipe vary among the operators in the Delaware Basin. For example, a recent well spudded on January 20, 2003 (Pogo Producing Company WBR Federal #9 well located in Lea County at T22S-R32E-Sec 13) provides the following as representative information:

- While drilling through the salt formation the mud pumping rate was 340 gallons/minute. The mud was a brine solution. Mr. Alan Means, a principal of Cambrian Management, suggested a 320 GPM pump rate (see Appendix D). The recommendation for DRSPALL is to sample from a uniform distribution of +/- 20% of 320 GPM, this gives, in SI units m^3/s :

Low	1.615E-02
Mean	2.018E-02
High	2.422E-02

- 4 ½" drill pipe was used that was rated at 16.60 lbs/foot. The internal diameter is 3.826" for the specific drill pipe used.
- The drill bit used to drill the salt formation was an 11" tricone bit with three #14 nozzles with the nozzles being ¼" i.d. Many times they will use a 12 ½" drill bit to drill the salt formation and it uses the same nozzle setup as the 11" bit.
- If a gas kick is encountered while drilling and everyone is attentive, the driller will notice a volume increase in the mud return rates and the well can be shut in within two minutes of encountering the gas kick. Because of all of the monitors, the driller can differentiate between air pockets, gas pockets, and brine pockets. In the case of an air pocket the standard procedure is to stop drilling but let the air vent out of the well, and when depleted, the drilling is continued. When encountering pressurized brine, if the flow rate is not too high, the mud-pumping rate is decreased to match the output (a barrel in-a barrel out) and drilling continues.

Parameter values thus identified for standard practices are:

Pipe outer diameter	0.114 m	(4.5 inch)
Pipe inner diameter	0.097 m	(3.826 inch)
Bit nozzle diameter	#14	(14/32 inch = 0.011m)
Bit nozzle number	3	(number of nozzles in tricone bit)

3.2 Stop Drilling Exit Volume Rate and Stop Pumping Exit Volume Rate

This section discusses the input parameters to DRSPALL, "stop drilling exit volume rate" and "stop pumping exit volume rate" that control drilling and mud pump shutoff in the event of a gas kick in a drilling intrusion of WIPP. While the code maintains the capability to exercise driller control of a blowout event, the bounding case of no intervention is assumed for all PA compliance calculations, as discussed below. Therefore, the stop drilling exit volume rate and stop pumping exit volume rate parameters are set so that the drilling and pumping continue uninterrupted throughout the run.

Background

Well control is an important safety consideration in oil and gas drilling operations. Typically, the drilling mud density is controlled to maintain a slightly "overbalanced" condition so that the mud pressure is always slightly higher than the fluid pressures in the formation. If the borehole suddenly passes through a high-pressure zone, the drill string can quickly become "underbalanced," with a resulting fluid pressure gradient driving formation fluids into the wellbore. This situation is known as a "kick," and is of great concern to the driller because a

violent kick can lead to a blowout of mud, gas, and oil from the wellbore, leading to equipment damage and worker injury.

Standard drilling practice is to watch diligently for kicks. The first indicator of a kick is typically an increase in mud return rate leading to an increase in mud pit volume (Frigaard and Humphries, 1997; Hughes, 2003). Down-hole monitors detect whether the kick is air, H₂S, or brine. If the kick fluid is air, the standard procedure is to stop drilling and continue pumping mud in order to circulate the air pocket out. If the mud return rate continues to grow after drilling has stopped and the driller believes that the kick is sufficiently large to cause damage, the well may be shut in by closing the blowout preventer. Once shut in, the well pressure may be bled off slowly and mud weight eventually increased and circulated to offset the higher formation pressure before drilling continues.

Implementation in DRSPALL

DRSPALL models an underbalanced system in which a gas kick is assured. Further, to obtain a bounding assumption, the kick proceeds with no intervention from the driller. The easiest and most extreme modeling case is to allow the drilling and pumping to continue during the entire kick and ensuing blowout event.

DRSPALL was built to allow some driller “control” over the well during a kick. Drilling and pumping may be switched off by setting a limit on the mud ejection rate at the top of the wellbore. Recall that mud ejection rate is usually the first clue to a driller that a kick has started. Mud exit volume rate at the outlet should equal the mud pump rate at the inlet during steady-state operation. A default value for the “stop drilling exit volume rate” of 0.1 m³/s, or about 2.5x the default pump rate of 0.038 m³/s was inserted. This value was problematic because bleed-off through the drilling damage Zone (DDZ) triggered drill shutoff in high-pressure cases before the bit reached the repository. In the sensitivity runs, we set this parameter to a constant 1000 m³/sec and thus preclude driller intervention prior to repository penetration. Although not an expected condition, this allows the analysis to continue such that a bounding result is obtained.

During scoping executions of DRSPALL the “stop pumping exit volume rate” was set to a constant high value of 1000 m³/s. The implication here is that while drilling may stop with a gas kick, current practice in the Delaware Basin is to circulate the gas out by mud pumping. If the kick is severe enough, the driller will stop pumping and engage the blowout preventer and shut the well in. Simulating a situation where the pumping is stopped but the well is left open does not correlate to standard drilling practices, and is consequently eliminated as a scenario for WIPP. As such, we choose not to exercise the “stop pumping exit volume rate” pump shutoff switch. In a severe spalling event, the time at which the drilling shuts down is not too important to ultimate releases because the failure surface proceeds ahead of the drillbit. The “stop pumping exit volume rate,” is thus set at 1000 m³/s so that all runs include pumping throughout because well shut-in logically follows pump shutoff, and shut-in does not model the spallings process.

Parameter name	Units	Value	Distribution
Stop drilling exit volume rate	m ³ /sec	1000	Constant
Stop pumping exit volume rate	m ³ /sec	1000	Constant

3.3 Drill Penetration Rate

This section documents the type of distribution and range of values selected for the rate at which a drill bit moves down through the Salado Formation in the DRSPALL model. Attachment 1 of CCA Appendix DEL entitled “typical oil or gas drilling sequence in the Delaware Basin” provides the typical procedure used to drill through the Salado Formation. The weight on the bit during drilling would range from 10,000 to 60,000 pounds (4,536 to 27,216 kg). The rotary speed on the drill bit is 70- to 75 revolutions per minute. The drilling fluid is saturated brine. The rate of drilling penetration is 35 to 70 feet (10.7 to 21.3 m) per hour. This calculates to approximately 5.93E-03 to 2.96E-03 m/s. In Appendix DEL Section 7.5 of the CCA it is stated that drilling rates of 50 to 60 feet per hour are typical when drilling through the Salado Formation according to the "analytical study of an inadvertent intrusion of the WIPP site" published by the New Mexico Junior College (1995). This calculates to approximately 4.23E-03 m/s to 5.08E-03 m/s. Thus a reasonable range of bit penetration rates is 5.93E-03 to 2.96E-03 m/s.

3.4 Solids Volume Fraction and Viscosity Exponent

This section documents the range of values selected for the maximum solids volume fraction and viscosity exponent used to calculate the viscosity of drilling mud loaded with cuttings and spalled waste solid in the DRSPALL model. The transport of solids suspended in the drilling fluid, known more generally as slurry transport, is an important factor controlling the dynamics of fluid flow in a borehole. In the extreme, too much solid in the suspension will increase viscosity sufficiently to interrupt or choke the flow. Laboratory experiments designed to simulate the flow of slurry mixtures up the annulus of a borehole give both qualitative and quantitative insight to the relationship between solids concentration and slurry viscosity. In particular relevance to the DRSPALL model is work published by Barree and Conway (1995), in which they measured the viscosity increase in the annulus of a model flow cell with volumetric solids concentrations varied from 0.007 to 0.65. Barree and Conway (1995) express their resulting function in the form:

$$\frac{\eta}{\eta_o} = \left(1 - \frac{w}{w_{\max}}\right)^s \quad (3.4.1)$$

where η denotes the apparent slurry viscosity, η_o denotes the clean fluid viscosity, w denotes volumetric solids concentration, w_{\max} is the maximum attainable solids concentration, and s is the solids viscosity exponent. The two unknowns to be empirically determined were thus w_{\max}

and s . They reported that the effective values of w_{\max} ranged from 0.59 to 0.64, while s ranged from -1.2 to -1.8 . No apparent change in the relationship was observed as a function of shear rate.

Computation of the wellbore fluid dynamics in DRSPALL requires evaluation of the mud viscosity in the annulus between the drillpipe and the borehole walls. DRSPALL uses the power law equation expressed above in Equation 3.4.1. For purposes of DRSPALL sensitivity studies, values of w_{\max} ranging from 0.59 to 0.64, and s ranging from -1.2 to -1.8 are selected.

Parameter name	Units	Low	High	Distribution
Solids volume fraction	-	0.007	0.65	Uniform
Viscosity exponent	-	-1.2	-1.8	Uniform

3.5 Drilling Damage Zone

This section discusses a parameter called the DDZ, which is idealized in Figure 3.2 as a cylinder of altered-permeability salt material in advance of the drill. It is expected that the zone near the interface of a drill approaching the repository will be quite complex. Firstly it is expected that some rock damage will occur as a result of the mechanical drilling action, as well as the circulation of mud in the hole. In addition, fluid pressure-generated fractures may be expected to propagate from the repository for those future states in which fluid pressures exceed lithostatic conditions. These fractures might be expected to exist in the country rock along discontinuities, such as the clay and anhydrite stringers which have been damaged and distorted during the room-closure process. High-pressure gas will migrate through these fractures into the wellbore along the unhealed zones at some distance above the repository roof. This complex process is represented in this model as an idealized damage zone between the roof of the disposal areas and the penetrating drillbit.

Gas flow through the DDZ is assumed to be governed by Darcy's Law. The boundary pressure on the well side is the pressure immediately below the bit. The flow area is assumed to consist of the bit cross-sectional area (also assumed to be the wellbore area). The boundary pressure on the repository side is the repository pressure. The main effect of this drilling damage zone is to allow fluid coupling between the repository gas and the wellbore to smooth the step function in pressure and flow rate that would occur if an instantaneous bit penetration of the repository were allowed to occur. These boundary conditions are expected to capture the more complex physical processes expected to occur during an actual drilling event.

Two parameters, axial length and permeability, are needed to describe the DDZ, which is modeled as a cylindrical zone directly below the bit with a diameter equal to the bit (See Figure 3.2). The axial length, or depth, of the DDZ is assumed to be one-bit radius ahead of the bit, or 0.16m. This assumption of one-bit radius represents a bounding case because leakage into the wellbore would be expected to begin over a much larger distance. The DDZ permeability is expected to be no greater than that of crushed waste, or $10^{-12.9} \text{ m}^2$ (we used 10^{-13} m^2), with a lower end being estimated at 10^{-15} m^2 .

Parameters for the DDZ are therefore:

Parameter name	Units	Low	High	Distribution
DDZ thickness	m	0.16	0.16	Constant
DDZ permeability	m ²	10 ⁻¹⁵	10 ⁻¹³	Loguniform

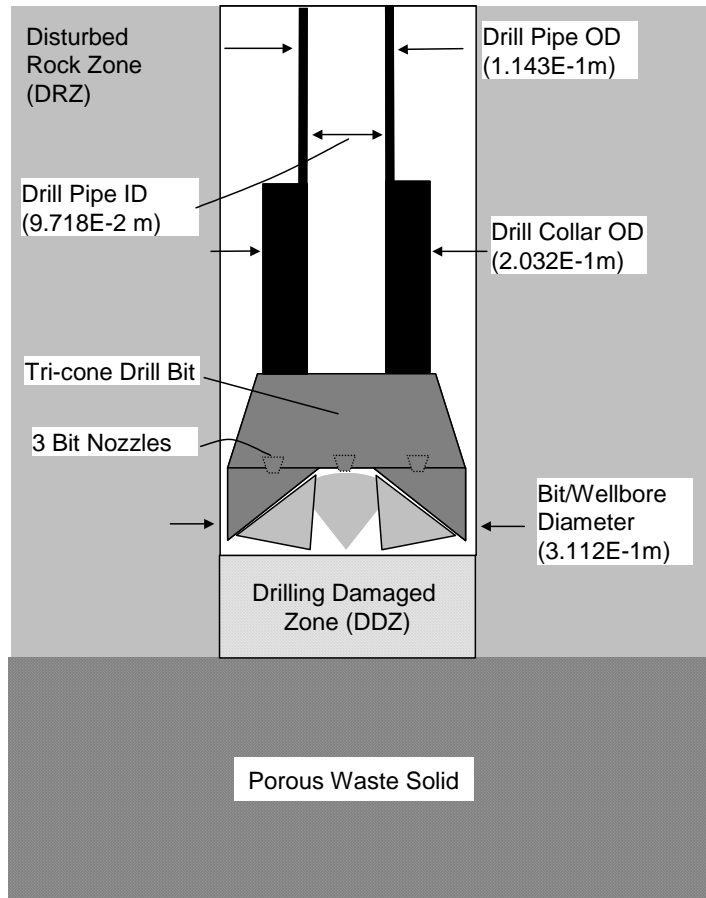


Figure 3.2. Schematic of drilling at bottom hole

3.6 Absolute Roughness of Pipe and Wellbore

This section documents the range of values selected for absolute roughness of the drill pipe and wellbore walls in the DRSPALL model.

Background

Fluid flow in the wellbore is influenced by the dissipative effect of friction between the moving fluids and stationary walls of the pipe and wellbore, leading to pressure loss along the direction of flow. The dominant properties controlling the magnitude of friction are pipe geometry (diameter, wall roughness), fluid viscosity, and fluid velocity. The frictional loss in DRSPALL is quantified using a standard formulation for pipe flow (Fox and MacDonald, 1985):

$$F = f \frac{\rho}{d_h} \frac{u^2}{2} \quad (3.6.1)$$

where F is the head loss per unit length of pipe (Pa/m), f is the Darcy friction factor, u is the fluid velocity, and d_h is the effective hydraulic diameter of the pipe section. For flow through circular pipe, d_h = inside diameter of pipe. For flow through the annulus, d_h = outer pipe diameter – inner pipe diameter.

The formula for friction factor is determined according to Reynolds number (Re):

$$\text{Re} = \frac{u \rho d_h}{\eta} \quad (3.6.2)$$

where η is the absolute viscosity of the drilling mud adjusted for gas and solids entrainment. In the laminar regime ($\text{Re} < 2100$) the friction factor is evaluated using (Fox and McDonald, 1985):

$$f = \frac{64}{\text{Re}} \quad (3.6.3)$$

while for the transitional and turbulent regime ($\text{Re} \geq 2100$), the Colebrook formulation is used (Fox and McDonald, 1985):

$$\frac{1}{\sqrt{f}} = 2.0 \log \left(\frac{\varepsilon/d_h}{3.7} + \frac{2.51}{\text{Re} \sqrt{f}} \right) \quad (3.6.4)$$

where ε is the absolute wall roughness.

Implementation in DRSPALL

For DRSPALL, representative values of absolute wall roughness (ε) are needed for the Colebrook friction loss equation (Eq. 3.6.4). The wall materials of interest are (1) the inner and outer walls of the steel drill pipe, and (2) the drilled wellbore through the host rock.

Fluid dynamics textbooks typically cite the work of Moody (1944), reproduced here in Figure 3.3., for determining friction factor and associated wall roughness in pipes constructed from standard engineering materials. Moody gives the roughness of commercial steel pipe as 1.5E-04 ft, which converts to 5.0E-05 m. Based on this, DRSPALL uses a steel pipe wall roughness of 5.0E-5 m for the interior of the drill pipe that feeds mud from the pump to the drill bit. Less well-defined is the roughness of the wellbore as it passes through the various formations from the land surface to the repository top. Conceptually, among the materials listed in Figure 3.3, the wellbore wall would most likely resemble concrete pipe, with a roughness ranging from 0.001 to 0.01 ft, which converts to 3.1E-04 to 3.1E-03 m. From the perspective of spillings waste release potential in the WIPP PA, smooth walls constitute a worst-case assumption. Factors that restrict the flow of mud up the wellbore, like high wall roughness, act to slow the rate of mud ejection during a blowout and actually result in lower spillings releases. In light of the uncertainty in actual wellbore wall roughness, it was decided to implement a range of values for wellbore wall roughness that represent a conservative assumption of relatively smooth walls. As such the spill model will use a loguniform distribution with a value of 3.1E-03 m (rough concrete) for the high end, and 5.0E-05 m (smooth steel) for the low end.

Parameter name	Units	Low	High	Distribution
Drill pipe absolute roughness	m	5×10^{-5}	5×10^{-5}	Constant
Wellbore absolute roughness	m	5×10^{-5}	3.1×10^{-3}	Loguniform

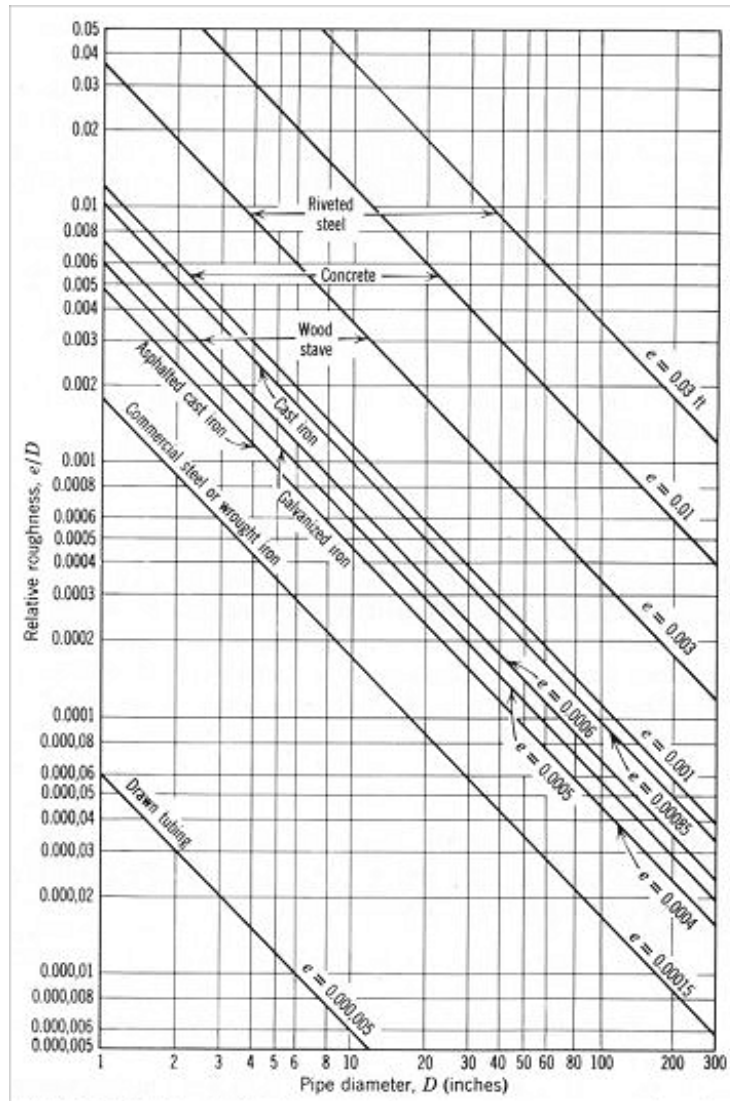


Figure 3.3. Diagram reproduced from Moody (1944) showing roughness values for common engineering materials.

4.0 OTHER FACTORS

4.1 Ergun Equation – Fluidized Bed Transport

The Ergun equation (Ergun, 1952) is used to model fluidized bed transport of disaggregated waste material. In the event that waste solids fail in tension, the material is moved from the repository to the wellbore by fluidized bed transport. In DRSPALL, the Ergun equation:

$$\frac{1.75}{a\phi^3} \left(\frac{d_p U_f \rho}{\eta} \right)^2 + 150 \left(\frac{1-\phi}{a^2 \phi^3} \right) \left(\frac{d_p U_f \rho}{\eta} \right) = \frac{d_p^3 \rho (\rho_w - \rho) g}{\eta^2} \quad (4.1.1)$$

is solved for minimum fluidization velocity, and compared with the superficial gas velocity (volume flow rate/cavity area) at the cavity wall. If the superficial gas velocity exceeds the minimum fluidization velocity, the failed solids are assumed fluidized, entrained, and added to the wellbore. The terms for Equation 4.1.1 are defined in Table 4.1.

Table 4.1 Nomenclature for Fluidization Calculations

Symbol	Definition	Units
a	Particle shape factor	--
d_p	Diameter of particles (mean)	m
g	Acceleration of gravity	m/s ²
U_f	Fluidization velocity	m/s
η	Viscosity of gas	kg /m s
ρ	Density of gas	kg/m ³
ρ_w	Density of waste solids	kg/m ³
ϕ	Porosity	--

Key assumptions in this model include particle diameter of disaggregated waste particles, particle shape, and porosity of bedded material to be fluidized. The Ergun equation requires a

uniform particle size, for which a value was sampled from a range of particle diameters (Section 3.5). The porosity of bedded material is assumed to be the same as for the intact waste material, which was discussed earlier in Section 2.6. Particle shape factor is discussed below.

Particle shape factor

The particle shape factor represents the sphericity of the disaggregated waste particles. Sphericity is defined as the surface area of a sphere with equivalent volume to the particle of interest, divided by the actual surface area of the particle. Recall that a sphere has the smallest surface area per unit volume of any geometric shape, so the numerator will always be smaller than the denominator in this fraction. In the limits, sphericity equals 1.0 for a sphere, and approaches zero for “flat” particles with high aspect ratios and consequently large surface area to volume ratios. The impact on the Ergun minimum fluidization velocity is that for a given characteristic particle diameter and density, particles with a lower sphericity will more readily fluidize. This occurs because fluidization of bedded particles occurs when the drag forces due to moving fluids (proportional to particle surface area) overcome the gravitational forces (proportional to particle volume) holding the bed in place. The functional relationship between minimum fluidization velocity and shape factor is illustrated in Figure 4.1 for the input parameter values shown in Table 4.2. See Appendix B for supporting calculations.

Table 4.2. Input parameter values for Ergun sensitivity to shape factor shown in Figure 4.1.

<i>Parameter</i>	<i>Value</i>
ϕ	0.575
ρ	11.74
ρ_w	2650
η	8.93E-06
d_p	1.0E-03

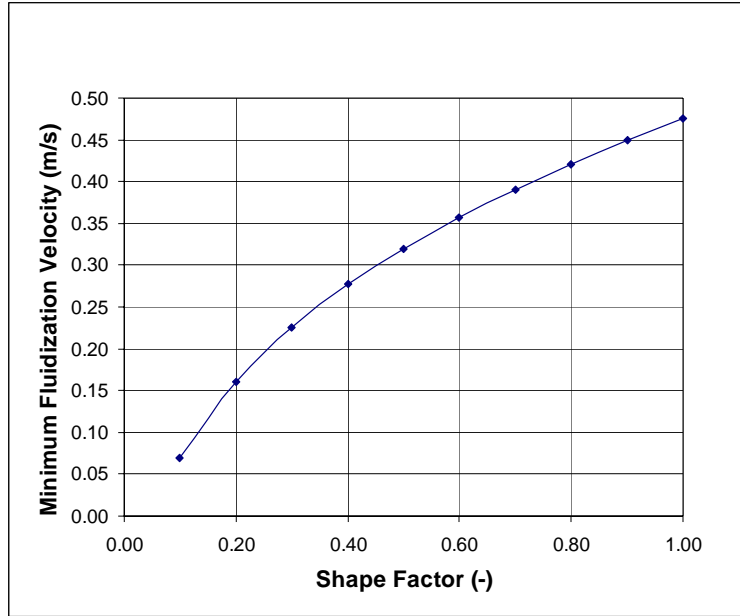


Figure 4.1. Minimum fluidization velocity calculated by Ergun’s equation (Eq. 4.1.1) as a function of shape factor, given input values shown in Table 4.2.

Figure 4.1 demonstrates that the minimum fluidization velocity can decrease as much as an order of magnitude with a similar decrease in shape factor from 1.0 to 0.1. In order to visualize the shape factor of non-spherical particles, some examples are given in Table 4.3 for cylinders with selected aspect ratios. For reference, a U.S. penny has an aspect ratio of about 19, with a resulting shape factor of 0.167.

Table 4.3 Shape factor calculated for cylinders with selected aspect ratios (diameter/height).

Property	Units	0.5	1.0	2.0	10.0	19.0
Aspect ratio	-	0.5	1.0	2.0	10.0	19.0
diameter	m	1.00E-03	1.00E-03	1.00E-03	1.00E-03	1.00E-03
height	m	2.00E-03	1.00E-03	5.00E-04	1.00E-04	5.26E-05
area	m ²	7.85E-06	4.71E-06	3.14E-06	1.88E-06	1.74E-06
volume	m ³	1.57E-09	7.85E-10	3.93E-10	7.85E-11	4.13E-11
equivalent sphere radius	m	7.21E-04	5.72E-04	4.54E-04	2.66E-04	2.14E-04
equivalent sphere area	m ²	3.27E-06	2.06E-06	1.30E-06	4.43E-07	2.89E-07
sphericity	-	0.416	0.437	0.413	0.235	0.167

Implementation in DRSPALL

The future state of the compacted, degraded WIPP waste is sufficiently uncertain that a range of particle shape factor will be used to represent the array of shapes of tensile-failed waste particles

subject to fluidization in the DRSPALL model. The upper limit is set to 1.0 as defined by geometry. The lower limit will be set to 0.1, representing a conservative assumption of flat, high-aspect ratio particles.

Parameter name	Units	Low	High	Distribution
Particle shape factor	-	0.1	1.0	Uniform

4.2 Atmospheric Pressure

Atmospheric pressure is a physical parameter used in DRSPALL modeling and will be treated as a constant. This section provides the required technical justification and appropriate source documentation for the parameter estimate. The WIPP Management and Operating Contractor (MOC) maintains a meteorological monitoring station approximately 600 m northeast of the WIPP Waste Handling Building. The main function of the station is to provide data for atmospheric dispersion modeling. The station measures and records wind speed and direction, temperature, barometric pressure, relative humidity, precipitation, and solar radiation. All meteorological data recorded since January 2000 have been validated according to the requirements of the Department of Energy Quality Assurance Program Document (DOE QAPD) for the time period January 2000 through June 2002 (WTS, 2002). The mean ground-surface atmospheric pressure and its standard deviation are 898.6 mbars and 5.2 mbars, respectively.

DRSPALL references atmospheric pressure to mean sea level rather than to mean ground-surface elevation. Correcting the observed mean ground-surface atmospheric pressure to mean sea level requires assumptions about local acceleration of gravity, temperature gradient, and humidity. If polytropic atmospheric conditions (i.e., temperature varies linearly with altitude) are assumed (a common assumption for altitudes less than 11,000 km (after Olsen, 1973)), then the pressure, p_1 , at any altitude (or elevation), z_1 , is related to a reference pressure, p_0 , and reference temperature, T_0 , through the following equation (Olsen, 1973):

$$\frac{p_1}{p_0} = \left[1 - g \frac{(n-1)}{n} \frac{z_1 - z_0}{RT_0} \right]^{\frac{n}{n-1}} \quad (4.2.1)$$

where n is known as the polytropic exponent, g is the acceleration of gravity, z_0 is the altitude (elevation) at the reference point, and R is a gas-specific constant.

For altitudes between 0 and 11,000 km, the polytropic exponent is 1.235 assuming a dry adiabatic atmosphere (Olsen, 1973). The acceleration of gravity varies both with latitude and altitude, but for mid-latitudes and altitudes between 0 and 11,000 km, the value is typically 9.79 m/s² (Olsen, 1973). The gas constant, R , for air is 287.1 m·N/kg·K and does not vary with temperature or pressure (Olsen, 1973). Using the U.S. standard atmosphere definition as the reference condition, $Z_0 = 0$ m (i.e., sea level) and $T_0 = 15$ C (288.15 K). Substituting these

reference values and the recommended values for n , g , and R into Equation 4.2.1 and assuming a WIPP ground-surface elevation, z_I , equal to 1037.326 m (Section 4.4), the atmospheric pressures at sea level (p_0) and at the WIPP ground surface (p_I) are related by:

$$\frac{p_I}{p_0} = 0.883 \quad (4.2.2)$$

Thus, from Equation 4.2.2, the corrected mean atmospheric pressure at sea level (p_0) is $p_I/0.883$ or $898.6 \text{ mbars}/0.883 = 1017.7 \text{ mbars}$ or $101,770 \text{ Pa}$.

4.3 Roof Elevation

During June – August 2000, the WIPP MOC performed a leveling survey of the rooms and access drifts comprising the newly-excavated disposal Panel 2. This survey established the roof and floor elevations at 10-ft station intervals for each of the seven disposal rooms and both the S2180 and S2520 drifts that provide access to the rooms. The elevation data for the survey was documented by Washington TRU Solutions LLC (WTS, 2002). The roof elevation data for Panel 2 used standard statistical estimators, as well as the average roof dip¹ both in the North – South and West – East directions. The mean roof elevation in Panel 2 is 385.31 m with a standard deviation of 0.77 m.

The mean roof elevation determined for Panel 2 is not an accurate representation of the roof elevation of the disposal area because of the prevailing dip at the WIPP and because future repository panels will be mined to Clay Seam G, thereby raising the roof 2.43 m. Therefore, to provide a best estimate of the average roof elevation in the disposal area, the mean roof elevation and dips determined from the Panel 2 survey data were used to extrapolate the roof elevations in panels yet to be excavated, as well as in existing Panel 1, using the horizontal distances between the center of Panel 2 and the centers of each of the other seven panels. For this calculation, the North-South and East-West separation distances between adjacent panels are set at 175 m and 525 m, respectively. The mean roof elevation for Panel 2 and the extrapolated roof elevations for the other seven panels are summarized in Table 4.4. Based on these values, the average roof elevation in the disposal area is 384.70 m and is the value recommended for the DRSPALL calculations. The standard deviation determined for the mean roof elevation of Panel 2, i.e., 0.77 m, is an appropriate estimator for the standard deviation of the average roof elevation in the disposal area.

¹ Disposal panels are excavated following the prevailing dip of the Salado Formation salt beds in the vicinity of the WIPP.

Table 4.4 Roof Elevations at the Center of Each WIPP Waste Disposal Panel

	Panel								
	1	2	3	4	5	6	7	8	Mean
Roof Elevation ^(a) (m)	388.18	385.31	382.44	379.57	381.22	384.09	386.96	389.83	384.70

(a) Panel 2 roof elevation is based on survey data. Roof elevations for other panels are extrapolated using Panel 2 roof dips and North-South and East-West panel separation distances of 175 m and 525 m, respectively.

4.4 Land Surface Elevation

The WIPP MOC performs annual leveling surveys of the land surface directly above the underground openings at the WIPP. These surveys support the WIPP subsidence-monitoring program and, as such, are conducted according to established procedures prepared in accordance with the DOE QAPD. Surface elevations are determined from ten loops containing 51 monuments and 14 National Geodetic Survey vertical control points. The surveys meet Second-Order Class II loop closure accuracies (i.e., $0.033 \text{ ft} \times \sqrt{\text{mile}}$ or better). Elevations are referenced to a monument located approximately 7,700 feet north of the most northerly boundary of the WIPP underground excavation. This location is considered to be far enough from the WIPP facility to be unaffected by excavation-induced subsidence expected directly above and near the WIPP underground. In practice, survey accuracy for all loops is consistently 0.003 ft or better, which exceeds the Second-Order Class II closure accuracy requirement by more than an order of magnitude. Adjusted elevations are determined for every monument/control point by proportioning the vertical closure error for each survey loop to the monuments/control points comprising the loop. The proportions are based on the number of instrument setups and distance between adjacent points within an individual loop.

In estimating a constant value for the elevation of the WIPP land surface, the 2002 data from the 32 benchmarks located directly above the waste panels were used (U.S. DOE, 2002). The mean surface elevation determined from the 31 active benchmarks located directly above the waste panels is 1,037.326m. This value is recommended for use in the DRSPALL calculations.

4.5 In Situ Stress

Creep properties of salt and the nontectonic setting of the Delaware Basin suggest the virgin in situ stress state at WIPP is isotropic. The rock column overlying the WIPP site is reasonably well characterized, such that the in situ stress can be estimated. Wawersik and Stone (1995), in concert with their hydraulic fracturing tests at the WIPP, expected the in situ stress to be 14.78 to 15.01 MPa. The inferred stress at the depth of their hydraulic fractures is 14.9 MPa. Although Wawersik and Stone (1995) encountered some variability, their field measurements were not substantially apart from the assumption that the vertical stress is a principal stress equal to the overburden stress and that the stress field was isotropic. Wawersik and Stone (1995) also dyed fracture patterns and observed multiple fracture patterns without preferred orientation beyond about 50 m from the boundary of nearby mine workings as opposed to strongly oriented fractures at smaller distances. Thus the far field stress beyond the influence of mining activities is assumed to be 14.9 MPa and isotropic.

4.6 Salt Density

Flow in the DRSPALL wellbore is treated as a compressible, viscous, multi-phase mixture of mud, gas, salt, and possibly waste solids. An equation of state relating pressure and density is used to complete the system of wellbore equations to calculate wellbore flow. The equation of state must account for the four possible mass components in the well: mud, salt, gas, and waste. In Appendix GCR Section 1.8 of the CCA, a value for the density of rock salt found in the WIPP horizons is given to be $2,180 \text{ kg/m}^3$. This value is an average value given at 25°C .

5.0 REFERENCES

- Baree, R.D, and Conway, M.W. 1995. Experimental and Numerical Modeling of Convective Proppant Transport, *Journal of Petroleum Technology* 47(3):216-222.
- CTAC. 1997. *Expert Elicitation on WIPP Waste Particle Diameter Size Distribution(s) during the 10,000-Year Regulatory Post-closure Period: Final Report*. Carlsbad, NM: U.S. DOE-Carlsbad Area Office.
- EPA (U.S. Environmental Protection Agency). 1996. 40 CFR Part 194: Criteria for the Certification and Re-Certification of the Waste Isolation Pilot Plant's Compliance with the 40 CFR Part 191 Disposal Regulations; Final Rule. *Federal Register*, Vol. 61, No. 28, pp. 5224 - 5245, February 9, 1996. Office of Air and Radiation, Washington, D.C. 1996.
- Ergun, S. 1952. *Chemical Engineering Progress*. 48:89.
- Fox, R.W., McDonald, A.T. 1985, *Introduction to Fluid Mechanics, 3rd Ed.*, John Wiley and Sons, New York.
- Frigaard, I.A. and N.L. Humphries. 1997. *High Penetration Rates: Hazards and Well Control – A Case Study: Proceedings, March 1997 Society of Petroleum Engineers/International Association of Drilling Contractors Drilling Conference*. SPE paper 37953. Amsterdam, Netherlands: Society of Petroleum Engineers.
- Hansen, F.D., M.K. Knowles, T.W. Thompson, M.B. Gross, J.D. McLennan, and J.F. Schatz. 1997. *Description and Evaluation of a Mechanistically Based Conceptual Model for Spall*. SAND97-1369. Albuquerque, NM: Sandia National Laboratories.
- Hansen, C., Leigh, C., Lord, D., and Stein, J. 2002. "BRAGFLO Results for the Technical Baseline Migration." Carlsbad, NM: Sandia National Laboratories. ERMS# 523209.
- Helton, J.C, J.E. Bean, J.W. Berglund, F. J. Davis, K. Economy, J.W. Garner, J.D. Johnson, R.J. MacKinnon, J. Miller, D.G. O'Brien, J.L. Ramsey, J.D. Schreiber, A. Shinta, L.N. Smith, D. M. Stoelzel, C. Stockman, and P. Vaughn. 1998. *Uncertainty and Sensitivity Analysis Results Obtained in the 1996 Performance Assessment for the Waste Isolation Pilot Plant*. Albuquerque, NM: Sandia National Laboratories
- Hughes, D. 2003. Drilling Related Questions. Memorandum to D. Lord attached as Appendix C.
- Jaeger, J. C. and N.G.W. Cook. 1976. *Fundamentals of Rock Mechanics*, Second Edition, John Wiley and Sons, New York, NY.

- Means, A. 2003. Typical Jet Size and Pump Rate in Delaware Basin. Memorandum to D. Lord attached as Appendix D.
- Moody, L.F. 1944. Friction Factors in Pipe Flow, Trans ASME 1944, 66-671-684.
- New Mexico Junior College. 1995. Analytical Study of an Inadvertent Intrusion of the WIPP Site, Hobbs, New Mexico.
- NRC. 1996. The Waste Isolation Pilot Plant: A Potential Solution for the Disposal of Transuranic Waste. Committee on the Waste Isolation Pilot Plant, Board on Radioactive Waste Management. Washington, DC: National Academy Press.
- Olson, R.M., 1973. *Essentials of Engineering Fluid Mechanics*. New York, NY: Intext Educational Publishers.
- Sandia National Laboratories. 1997. *Chemical Condition Model: Results of the MgO Backfill Efficacy Investigation*, April 23, 1997.
- Stein, J., and Zelinski, W. 2003a. "Analysis Plan for the Testing of a Proposed BRAGFLO Grid to be used for the Compliance Recertification Application Performance Assessment Calculations." AP-106. Carlsbad, NM: Sandia National Laboratories. ERMS# 525236.
- Stein, J., and Zelinski, W. 2003b. "Analysis Report for: Testing of a Proposed BRAGFLO Grid to be used for the Compliance Recertification Application Performance Assessment Calculations." Carlsbad, NM: Sandia National Laboratories. ERMS# 526868.
- Stone, C.M. 1997. *Final Disposal Room Structural Response Calculations*. SAND97-0795. Albuquerque, NM: Sandia National Laboratories.
- U.S. DOE. 1996. Title 40 CFR Part 191 Compliance Certification for the Waste Isolation Pilot Plant. DOE/CAO-1996-2184. Carlsbad, NM: U.S. Department of Energy.
- U.S. DOE. 2002. *WIPP Subsidence Monument Leveling Survey 2002*. DOE/WIPP 03-2293. Carlsbad, NM: U.S. Department of Energy.
- U. S. DOE. 2002. Delaware Basin Monitoring Annual Report. DOE/WIPP-99-2308 Rev. 3. Carlsbad NM: U. S. Department of Energy.
- Wang, Yifeng. 1997. Estimate WIPP waste particle waste sizes based on expert elicitation results: Revision 1. Memorandum to Margaret S.Y. Chu and Mel G. Marietta, August 5, 1997. WPO#46936. Albuquerque, NM: Sandia National Laboratories.
- Warpinski, N.R. and L.W. Teufel. 1992. Determination of the Effective Stress Law for Permeability and Deformation in Low-permeability Rocks. SPE Formation Evaluation.

- Wawersik, W. R. and C. M. Stone. 1985. *Application of Hydraulic Fracturing to Determine Virgin In Situ Stress State around Waste Isolation Pilot Plant--In Situ Measurements*. SAND85-1776. Albuquerque, NM: Sandia National Laboratories.
- WEC. 1994. "Backfill Engineering Analysis Report Waste Isolation Pilot Plant." Carlsbad, NM: Westinghouse Electric Company, Waste Isolation Division.
- WTS. 2002. "Compliance Recertification Application Monitoring Data." Vol. 2. Carlsbad, NM: Washington TRU Solutions.
- WTS. 2002. "Compliance Monitoring Application Monitoring Data." Vol. 2. Carlsbad, NM: Washington TRU Solutions.

6.0 ACKNOWLEDGEMENT

Sandia is a multiprogram laboratory operated by Sandia Corporation, a Lockheed Martin Company, for the United States Department of Energy's National Nuclear Security Administration under Contract DE-AC04-94AL85000.

This research is funded by WIPP Programs administered by the U.S. Department of Energy.

APPENDIX A

Master Table of DRSPALL Physical Parameters

Table A.1 below lists all of the physical parameters called by DRSPALL in a typical execution. Included are data retrieved directly from the WIPP PA database, output data from other codes (i.e., BRAGFLO), and the “new” values discussed in the text of this spallings model parameter justification report. The column heading “Source” gives the source of the parameter from the perspective of DRSPALL. In order to run DRSPALL stand-alone during sensitivity studies, the range and distribution of uncertain parameters are defined in accordance with this table and assigned to unique input sets or “vectors” selected using a Latin Hypercube Sampling (LHS) technique. Stand-alone runs that use the “default” input values use the median values.

Table A.1 Master Table of Physical Parameters Called in a Typical DRSPALL Execution

	<i>Parameter</i>	<i>Units</i>	<i>Source</i>	<i>MATERIAL</i>	<i>PARAMETER</i>	<i>Distribution</i>	<i>Median</i>	<i>Low</i>	<i>High</i>
1	Land Elevation	m	NEW			Constant	1.0373E+03		
2	Repository Top	m	NEW			Constant	3.8470E+02		
3	DRZ Permeability	m ²	CCA PA database	DRZ_1	PRMX_LOG	LogUniform	1.1220E-16	3.9811E-20	3.1623E-13
4	Initial Gas Pressure	Pa	BRAGFLO			Uniform	1.1450E+07	8.0000E+06	1.4900E+07
5	Far-Field In-Situ Stress	Pa	NEW			Constant	1.4900E+07		
6	Porosity	-	BRAGFLO			Uniform	5.0500E-01	3.5000E-01	6.6000E-01
7	Permeability	m ²	NEW RANGE			LogUniform	2.4000E-13	2.4000E-14	2.4000E-12
8	Biot Beta	--	NEW			Constant	1.0000E+00		
9	Poisson's Ratio	--	NEW			Uniform	3.9000E-01	3.5000E-01	4.3000E-01
10	Cohesion	Pa	NEW			Constant	1.4000E+05		
11	Friction Angle	deg	NEW			Constant	4.5800E+01		
12	Tensile Strength	Pa	NEW VALUE			Uniform	1.4500E+05	1.2000E+05	1.7000E+05
13	Particle Diameter	m	NEW			LogUniform	1.0000E-02	1.0000E-03	1.0000E-01

14	Gas Viscosity	Pa*s	CCA PA database	H2	VISCO	Constant	8.9339E-06		
15	Mud Density	kg/m ³	CCA PA database	DRILLMUD	DNSFLUID	Cumulative	1.2100E+03	1.1400E+03	1.3800E+03
16	Mud Viscosity	Pa*s	CCA PA database	DRILLMUD	VISCO	Cumulative	1.1000E-02	5.0000E-03	3.0000E-02
17	Pipe roughness	m	NEW			Constant	5.0000E-05		
18	Wellbore roughness	m	NEW			Loguniform	3.9370E-04	5.0000E-05	3.1000E-03
19	Max. Solids Vol. Fraction	--	NEW			Uniform	6.1500E-01	5.9000E-01	6.4000E-01
20	Solids Viscosity Exponent	--	NEW			Uniform	-1.5000E+00	-1.8000E+00	-1.2000E+00
21	Bit Diameter	m	CCA PA database	BOREHOLE	DIAMMOD	Constant	3.1115E-01		
22	Pipe Diameter	m	CCA PA database	BOREHOLE	PIPED	Constant	1.1430E-01		
23	Collar Diameter	m	CCA PA database	BOREHOLE	COLDIA	Constant	2.0320E-01		
24	Pipe Inside Diameter	m	NEW			Constant	9.7180E-02		
25	Collar Length	m	CCA PA database	BOREHOLE	L1	Constant	1.8288E+02		
26	Drilling Rate	m/s	NEW			Uniform	4.4450E-03	2.9633E-03	5.9267E-03
27	Mud Pump Rate	m ³ /s	NEW			Uniform	2.0181E-02	1.6145E-02	2.4218E-02
28	DDZ Thickness	m	NEW			Constant	1.6000E-01		
29	DDZ Permeability	m ²	NEW			LogUniform	1.0000E-14	1.0000E-15	1.0000E-13
30	Stop Drilling Exit Vol Rate	m ³ /s	NEW			Constant	1.0000E+03		
31	Stop Pumping Exit Vol rate	m ³ /s	NEW			Constant	1.0000E+03		
32	π	-	CCA PA database	REFCON	PI	Constant	3.1416E+00		
33	Atmospheric pressure	Pa	NEW			Constant	1.0177E+04		
34	Gravitational constant	m/s ²	CCA PA database	REFCON	GRAVACC	Constant	9.8066E+00		
35	Water Compressibility	1/Pa	CCA PA database	BRINESAL	COMPRES	Constant	3.1000E-10		
36	Gas Constant	J/kg K	CCA PA database	BLOWOUT	RGAS	Constant	4.1160E+03		
37	Repository Temperature	K	CCA PA database	BLOWOUT	TREPO	Constant	3.0000E+02		
38	Waste Density	kg/m ³	CCA PA database	BLOWOUT	RHOS	Constant	2.6500E+03		
39	Salt Density	kg/m ³	NEW			Constant	2.1800E+03		
40	Shape Factor	--	NEW			Uniform	5.5000E-01	1.0000E-01	1.0000E+00
41	Bit Nozzle Number	--	NEW			Constant	3.0000E+00		
42	Bit Nozzle Diameter	m	NEW			Constant	1.1113E-02		

APPENDIX B

Spreadsheet Calculations for Ergun Shape Factor

The Ergun (1952) equation (Eq. 4.1.1) for determining minimum fluidization velocity U_f was solved as a function of shape factor (a) for selected values from 0.1 to 1.0 in order to demonstrate the Ergun model sensitivity to uncertainty in this input parameter. Note that Eq. 4.1.1 is a quadratic equation that may be solved for U_f using the convention:

$$AU_f^2 + BU_f + C = 0 \tag{B.1}$$

$$U_f = \frac{-B \pm \sqrt{B^2 - 4AC}}{2A} \tag{B.2}$$

The following excerpt from a spreadsheet demonstrates the method used to generate Figure 4.1.

Table B.1 Supporting spreadsheet calculations for Figure 4.1.

Shape Factor

HYDROGEN										
porosity	5.75E-01									
gas density	1.17E+01									
waste density	2.65E+03									
gas viscosity	8.93E-06									
gas pressure	1.45E+07									
particle diameter	1.00E-03									
shape factor	1.00E-01	2.00E-01	3.00E-01	4.00E-01	5.00E-01	6.00E-01	7.00E-01	8.00E-01	9.00E-01	1.00E+00
a	1.59E+08	7.95E+07	5.30E+07	3.98E+07	3.18E+07	2.65E+07	2.27E+07	1.99E+07	1.77E+07	1.59E+07
b	4.41E+07	1.10E+07	4.90E+06	2.75E+06	1.76E+06	1.22E+06	9.00E+05	6.89E+05	5.44E+05	4.41E+05
c	-3.81E+06									
b ² -4ac	4.37E+15	1.33E+15	8.31E+14	6.13E+14	4.88E+14	4.05E+14	3.47E+14	3.03E+14	2.69E+14	2.42E+14
fluidization vel	6.91E-02	1.60E-01	2.26E-01	2.77E-01	3.19E-01	3.57E-01	3.90E-01	4.21E-01	4.49E-01	4.76E-01

APPENDIX C

Personal Communication from David Hughes to David Lord regarding current drilling practices in Delaware Basin.

From: Hughes, Dave - WRES [Dave.Hughes@wipp.ws]

Sent: Thursday, January 30, 2003 2:11 PM

To: Lord, David - SNL

Subject: Drilling Parameters

Dave,

Because of all of the variables associated with drill bits and drill pipe, all I would be able to provide to you would be a range of numbers, leaving you to pick at random numbers to use in your model. This morning I met Eldon Grant, the Pogo Producing Co. drilling representative at the WBR Federal #9 well located in Lea County at T22S-R32E-Sec 13. This well was spudded on Jan 20, 2003 and drilling continues below the 7,000 foot depth. I asked Mr. Grant the specifics on this particular well to get the exact numbers you require for your model.

1. While drilling through the salt formation the mud pumping rate was 340 gallons/minute. The mud was a brine solution.
2. 4 ½" drill pipe was used that was rated at 16.60 lbs/foot. The internal diameter is 3.826 for the specific drill pipe used.
3. The drill bit used to drill the salt formation was an 11" tricone bit with three #14 nozzles with the nozzles being ¼" i.d. Mr. Grant informed me that many times they will use a 12 ½" drill bit to drill the salt formation and it uses the same nozzle setup as the 11" bit.
4. If a gas kick is encountered while drilling and everyone is doing their job, the driller will notice a volume increase on the mud return rates and the well can be shut in within two minutes of encountering the gas kick. Because of all of the monitors for H₂S on the rigs the driller can differentiate between air pockets, gas pockets, and brine pockets. Mr. Grant said that in case of an air pocket the standard procedure is to stop drilling but let the air vent out of the well, when depleted, the drilling is continued. When encountering pressurized brine if the flow rate is not too high the mud pumping rate is decreased to match the output, in other words, "a barrel in-a barrel out" and drilling continues.

I will put together a hard copy of the above information and sent it to you via snail mail next week. If I can help you out in any other way feel free to call at anytime.

David L. Hughes
Delaware Basin Drilling Surveillance Program
505-234-7342
dave.hughes@wipp.ws

APPENDIX D

Personal Communication from Alan Means to David Lord re: typical jet size and pump rate in Delaware Basin

From: Alan Ameans [ameans@cambrianmgmt.com]

Sent: Tuesday, March 04, 2003 8:49 AM

To: Lord, David L

Cc: Steve Melzer

Subject: 12 1/4" bit jets

Mr. Lord

The typical jet size on bits in the 12 1/4" hole is ranges from 3-12's to 3-14's. The typical pump rate is 320 gpm. Some have taken the pump rates higher however that usually results in hole wash out problems in the salt sections. I hope that I have answered your question. I assume that you got my name from Mr. Melzer. I would like to introduce you to Cambrian Management, Ltd we are a project management company specializing in oil and gas operations, drilling and completions. If you would like more information please visit our web site at www.cambrianmgmt.com.

Thanks

Alan D. Means, PE
Cambrian Management, Ltd